JOURNAL OF STRUCTURAL BIOLOGY 111, 17–21 (1993)

Direct Visualization of Myosin Filament Symmetry in Tarantula Striated Muscle by Electron Microscopy

RAÚL PADRÓN,* JOSÉ REINALDO GUERRERO,* LORENZO ALAMO,* MARISTELA GRANADOS,* NORBERTO GHERBESI,† AND ROGER CRAIG†

*Laboratorio de Biología Estructural, Instituto Venezolano de Investigaciones Cientificas (IVIC), Apdo 21827, Caracas 1020A, Venezuela; and †Department of Cell Biology, University of Massachusetts Medical School, 55 Lake Avenue North, Worcester, Massachusetts 01655

Received May 20, 1993, and in revised form August 2, 1993

Chemically demembranated bundles of fibers from tarantula leg muscle were rapidly frozen in the relaxed state and freeze-substituted in the presence of tannic acid. Electron micrographs of thin transverse sections of freeze-substituted specimens frequently showed four clear, regularly organized projections (crossbridges) protruding from the backbones of the myosin filaments and partially wrapping around the filament surface. The rotational power spectra of individual filaments showed a peak at $N = 4$. Alignment and averaging of the images using correlation methods confirmed the fourfold symmetry and the slewed configuration of the crossbridges on the filament surface. These observations directly reveal essential features of the low-resolution three-dimensional helical reconstruction of negatively stained tarantula filaments calculated previously (R. A. Crowther, R. Padrón, and R. Craig, 1985, *J. Mol. Biol.* 184, 429–439).

INTRODUCTION

Muscle contraction occurs by the sliding of the thick filaments past the thin filaments, generated by cyclic interaction of the heads of myosin molecules with actin molecules. In order to understand the molecular basis of muscle contraction, it is necessary to determine the structure not only of the actin–myosin interface but also of the supportive framework, the thick and the thin filaments. Thick filament structure has been studied in detail by negative staining and cryoelectron microscopy of isolated filaments observed in muscle homogenates (Stewart *et al.*, 1981, 1985; Kensler and Levine, 1982; Vibert and Craig, 1983; Crowther *et al.*, 1985; Kensler and Stewart, 1983, 1986; Stewart and Kensler, 1986; Vibert, 1992). However, in order to study the structure of the thick filaments directly in the sarcomere, where contraction occurs, a sectioning technique is required. Sectioning of muscle rapidly frozen under relaxing conditions and then freeze-substituted and embedded has proved to be a powerful method for preserving the native helical array of crossbridges in frog (Padrón and Craig, 1989; Lepault *et al.*, 1991; Craig *et al.*, 1992) and tarantula (Padrón *et al.*, 1992) striated muscle. Transverse sections of scallop striated muscle processed in this way have revealed directly the number and conformation of crossbridges in the myosin filaments (Craig *et al.*, 1991). Here, we use this approach to study the crossbridge arrangement in sections of tarantula leg muscle, a muscle which has previously been studied by X-ray diffraction (Wray, 1982; personal communication; Padrón *et al.*, 1991) and by 3D reconstruction of negatively stained filaments (Crowther *et al.*, 1985). This muscle is of special interest as it is a striated muscle exhibiting myosin-linked regulation controlled by phosphorylation (Lehman and Szent-Györgyi, 1975; Craig *et al.*, 1987; Padrón *et al.*, 1991). Preliminary reports of this work have been published elsewhere (Guerrero *et al.*, 1992; Alamo *et al.*, 1992).

MATERIALS AND METHODS

Specimen Preparation

Chemically skinned bundles of fibers from the leg muscles of tarantulas (Brachypelma sp.) were rapidly frozen on a liquid helium-cooled copper block and then freeze-substituted in acetone containing tannic acid, followed by acetone containing OsO_4, as described by Padrón *et al.* (1992). Transverse sections were cut with a 45° Diatome diamond knife on a Reichert Ultracut E ultramicrotome. The specimen advance was set at the thinnest setting that produced a section with each cut, generally 30 to 50 nm. Sections were stained with uranyl acetate and lead citrate (Reynolds, 1963) and examined at 80 kV in a JEOL 100CX electron microscope or at 100 kV in a Hitachi H-500 electron microscope. Magnifications were calibrated using negatively stained tropomyosin paracrystals, repeat 39.5 nm (Caspar *et al.*, 1969).

Image Analysis

Single filaments from selected transverse sections were digitized on a raster corresponding to a 0.4-nm sampling of the original specimen as described by Craig *et al.* (1991). Filament images were classified into two separate groups depending on

1047-8477/93 $5.00

whether the crossbridge slew was clockwise or counterclockwise; the counterclockwise images were then mirrored digitally to be clockwise. The centering and slew of each filament was checked using the rotational filtering procedure (Crowther and Amos, 1971). Correlation coefficients, calculated at 1-degree intervals, and correlation averaging were carried out as described by Craig *et al.* (1991).

RESULTS

In ultrathin transverse sections (dark gray interference colors), myosin filaments (selected in the H-zone to avoid the presence of actin filaments) frequently showed four structures projecting from the surface of the filament backbone, which itself was frequently square in profile (Fig. 1). These projections were evenly spaced and extended up to a radius of 21.2 ± 2.5 nm (mean ± standard deviation of mean, $n = 36$). The maximum length of the projections above the surface of the backbone, viewed in transverse projection, was 9.9 ± 2.5 nm ($n = 36$). The projections often wrapped slightly around the filament axis (Figs. 1 and 2), sometimes in a clockwise and sometimes in a counterclockwise direction, depending on whether the filament was viewed toward or away from the bare zone (see Craig *et al.*, 1991). Some projections showed larger mass at high radius, with a narrow connecting neck (Figs. 2a, 2c, 2d, and 2g), while others were wider close to the backbone.

When the projections were sufficiently clearly defined to be counted, the number observed was 4. In about 81% of the cases, the four projections were similar in size, while about 19% appeared to show three bigger projections and a small one (Fig. 1). The latter appearance may result from filaments that have not been precisely transversely cut (see Craig *et al.*, 1991). We conclude that the rotational symmetry of the crossbridge arrangement, at least in the majority of filaments, is 4. This was confirmed in

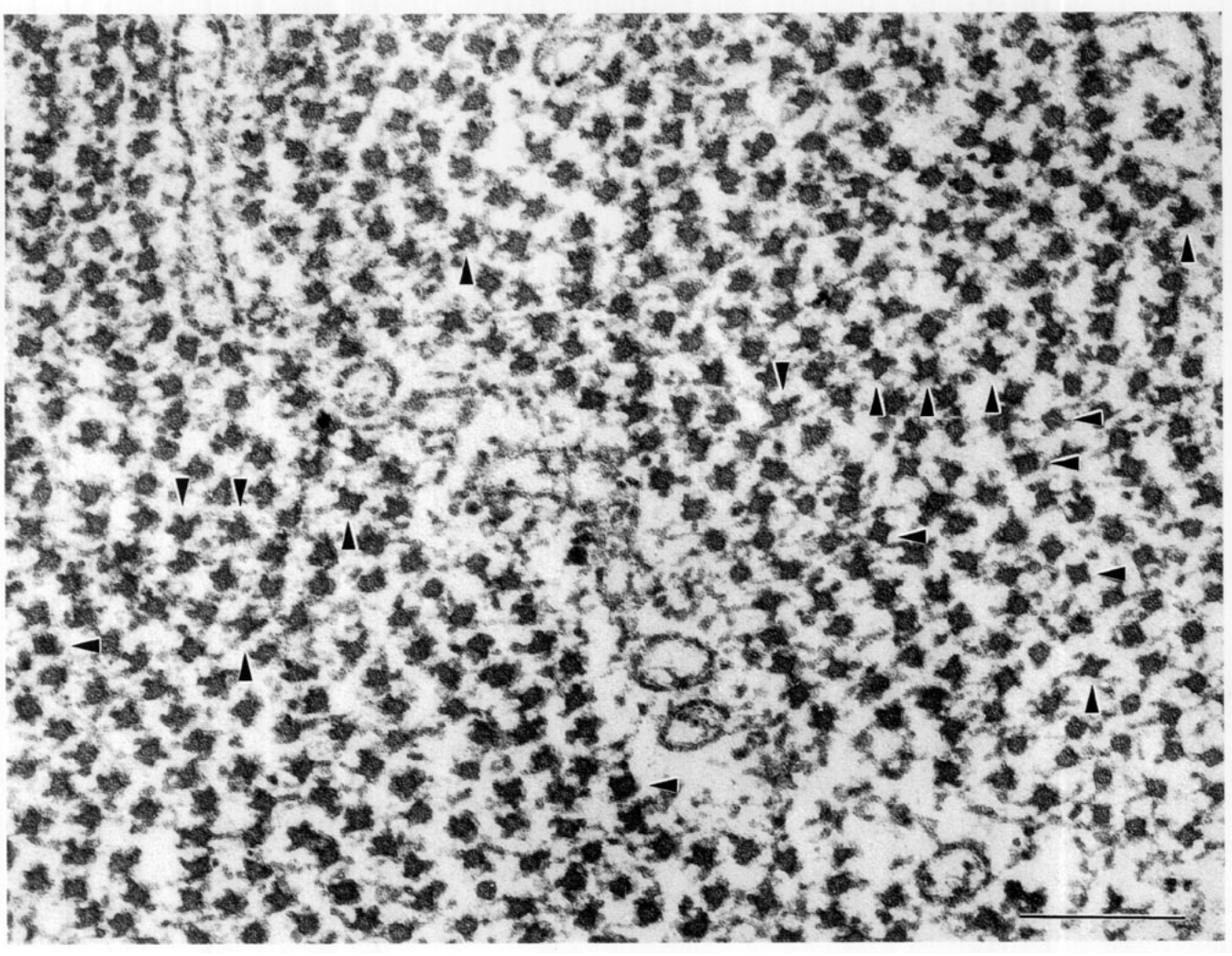

FIG. 1. Ultrathin transverse section of skinned, relaxed tarantula muscle, rapidly frozen and freeze-substituted in the presence of tannic acid, showing a fourfold arrangement of projections (crossbridges) in many filaments in the H-zone and overlap zone (arrowheads pointing up). Arrowheads pointing to the left show filaments with square backbone. Arrowheads pointing down show thick filaments with three bigger and one smaller protruding feature. Bar, 200 nm.

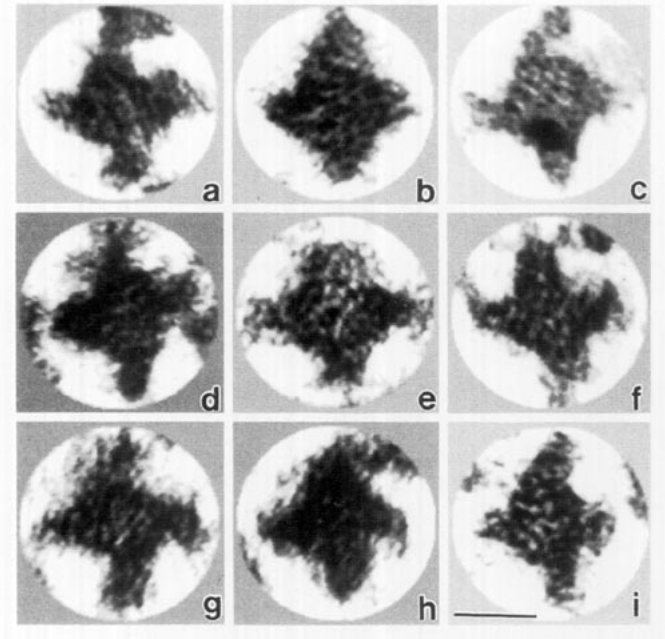

FIG. 2. Gallery of digitized images of nine selected myosin filaments used in the correlation analysis. The filaments are shown after centering and in the orientation that produced the maximum correlation coefficient when compared with the reference filament shown in (a). (a) Reference image; (b–i) filaments digitized from the same micrograph. Bar, 20 nm.

a more objective way by calculation of the correlation coefficient between different filaments, which showed four maxima, approximately equal in spacing and magnitude, in a full rotation of 360 degrees (Fig. 3), consistent with four similar projections spaced evenly around the circumference.

Image averaging was carried out using 20 selected

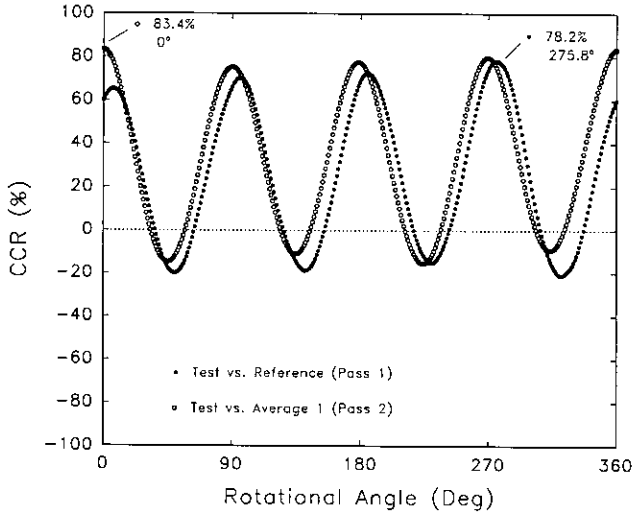

FIG. 3. Plot of cross-correlation coefficient (CCR, %) against rotation angle (in degrees) of a test filament against a reference filament. In pass 1, reference filament is filament "a" of Fig. 2. In pass 2, reference filament is first round average ("average 1" of Fig. 4). On pass 1, a maximum CCR of 78.2% is obtained for 275.8°, whereas on pass 2 a greater maximum (83.4%) is obtained, at 0°.

filaments, which by eye showed four clearly resolved projections (nine examples are shown in Fig. 2). Before averaging, the filaments were centered and then rotationally aligned against a reference (Fig. 4a) to maximize their correlation coefficient (Fig. 3). The average image (Figs. 4b and 4c) showed similar features to those already described for the majority of filaments: a fourfold arrangement of crossbridges partially slewed around the axis, generally wider close to the backbone and tapering at higher radius.

The rotational power spectrum of individual filaments and of the first and second averages had a peak at $N = 4$ (Fig. 5), again giving objective support to a fourfold rotational symmetry. The images after rotational filtering with fourfold symmetry imposed showed similar features to the unfiltered images (Fig. 6).

DISCUSSION

In this paper we have taken advantage of the close to *in vivo* preservation of striated muscle that is provided by the rapid freezing, freeze-substitution technique (Padrón *et al.*, 1988, 1992; Padrón and Craig, 1989; Craig *et al.*, 1991, 1992) to visualize directly the rotational symmetry of the crossbridge arrangement and the crossbridge structure in tarantula muscle.

The thinnest sections that we cut (~30 nm) must contain about two levels of myosin crossbridges (spaced 14.5 nm apart). A transverse projection of a 30-nm length of the three-dimensional reconstruction of negatively stained tarantula filaments (Crowther *et a.*, 1985) shows that the fourfold symmetry should still be visible at this thickness (Alamo and Padrón, unpublished data), as we observe. This is because the two crossbridge levels are rotated by only 30° with respect to each other and thus do not give rise to a continuous distribution of mass around the circumference of the thick filament backbone. In some images the myosin crossbridges were particularly well defined, suggesting that in some cases the part of the filament nearest to the section surface may have been preferentially stained, presumably due to incomplete penetration of stain through the section, thus revealing only one of the two crossbridge levels.

Each projection extending from the surface of the

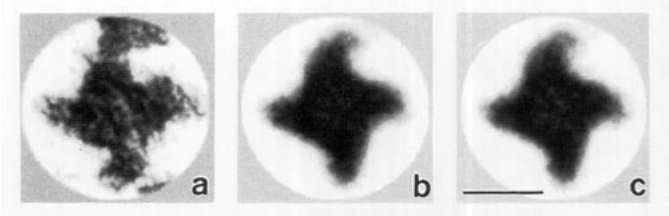

FIG. 4. (a) Reference image; (b) average image of 20 filaments ("average 1") oriented against the reference image shown in (a); (c) average image of the same 20 filaments ("average 2") oriented against average 1. Bar, 20 nm.

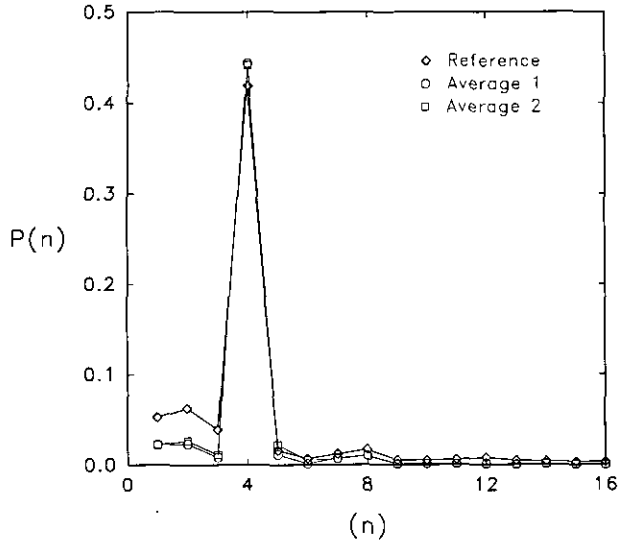

FIG. 5. Rotational power spectra of the reference image (Fig. 4a), average 1 image (Fig. 4b), and average 2 image (Fig. 4c). n, rotational symmetry; P (n) rotational power spectrum.

myosin filaments presumably represents 1–2 pairs of myosin heads, depending on the penetration of the stain into the section. In most cases the number of crossbridges seen in very thin sections was 4; this number was also implied by the plot of correlation coefficient vs rotation angle (Fig. 3) and by the rotational power spectra (Fig. 5) of individual and averaged filaments. The average thick filament (Figs. 4b and 4c) and the rotationally filtered images (Figs. 6b and 6c) clearly showed that the four projections were partially wrapped around the filament axis.

The rotationally averaged filament approximately superimposes on the transverse projection of one level of crossbridges in the 3D helical reconstruction computed from longitudinal images of negatively stained tarantula filaments (Crowther *et al.*, 1985) and from longitudinal sections of freeze-substituted tarantula muscle (Padrón *et al.*, 1992; Alamo *et al.*, in preparation). The fourfold symmetry and slewing were both essential features of the computed reconstruction. Here these features are seen directly, adding support to the computed structure without any assumptions of helical symmetry or deducing the rotational symmetry from the Fourier transform.

The backbone of freeze-substituted filaments sometimes showed a square profile, consistent with the fourfold arrangement of crossbridges. However, for reasons we do not understand, other filaments intermingled with the square ones were fairly circular. The fact that in thicker sections the backbone of the filaments was often more circular in profile and not square implies that the square profile is probably twisting as one moves along the filament. In specimens conventionally fixed in the presence of tannic acid (Guerrero and Padrón, 1992) we have been unable to see the square profile (although an internal core with fourfold symmetry was seen). This may be due to the better preservation attainable by the rapid freezing, freeze-substitution method. We are currently trying to improve preservation and resolution of the internal features of the backbone by negatively staining transverse cryosections of tarantula muscle.

The results we have presented here are a further demonstration that the rapid freezing/freeze-substitution technique preserves structure well at the molecular level (in this case the labile arrangement of relaxed crossbridges) and is thus a valid technique not only for the determination of macromolecular structure but also for the trapping of transiently occurring structures (e.g., structural intermediates of the crossbridge cycle). Using these relaxed images as a starting point, we hope to use rapid freezing to study changes in the crossbridges that occur when these filaments are switched on by phosphorylation of their regulatory light chains (Craig *et al.*, 1987; Padrón *et al.*, 1991).

FIG. 6. (a) Reference image (Fig. 4a); (b) average 1 image (Fig. 4b); (c) average 2 image (Fig. 4c), all after rotational filtering with fourfold symmetry imposed. Bar, 20 nm.

We are especially grateful to Dr. R. A. Crowther for helping us initially with the cross-correlation analysis. We thank Ing. Pedro Uman for help with image processing and Ms. Marie Picard Craig, Mr. Jose Luis Bigorra, and Mr. Pedro Medina for photographic help. One of us (J.R.G.) acknowledges the support of the Advanced Studies Center (CEA) of the Venezuelan Institute for Scientific Research (IVIC) and the Gran Mariscal de Ayacucho Foundation (FGMA) of Venezuela. This work was supported by grants from the NIH (AR34711 to R.C.), CONICIT (S1-2006 to R.P.), MDA (to R.C. and to R.P.) and by a US–Venezuela Cooperative Research Grant from NSF (INT8715515 to R.C.) and CONICIT (to R.P.).

REFERENCES

Alamo, L., Guerrero, J. R., Granados, M., Gherbesi, N., Craig, R., and Padrón, R. (1992) Direct determination of myosin filament symmetry in tarantula striated muscle by rapid freezing and freeze-substitution, *in* Megias-Megias, L., Rodriguez-Garcia, M. I., Rios, A., and Arias, J. M. (Eds.), Proceedings of the 10th European Congress on Electron Microscopy, Vol. III, pp. 53–54, Universidad de Granada, Granada.

Caspar, D. L. D., Cohen, C., and Longley, W. (1969) Tropomyosin: Crystal structure, polymorphism and molecular interactions. *J. Mol. Biol.* 41, 87–107.

Craig, R., Padrón, R., and Kendrick-Jones, J. (1987) Structural changes accompanying phosphorylation of tarantula muscle myosin filaments. *J. Cell Biol.* 105, 1319–1327.

Craig, R., Padrón, R., and Alamo, L. (1991) Direct determination

of myosin filament symmetry in scallop striated adductor muscle by rapid freezing and freeze-substitution. *J. Mol. Biol.* **220**, 125–132.

Craig, R., Alamo, L., and Padrón, R. (1992) Structure of the myosin filaments of relaxed and rigor vertebrate striated muscle studied by rapid freezing electron microscopy. *J. Mol. Biol.* **228**, 474–487.

Crowther, R. A., and Amos, L. (1971) Harmonic analysis of electron microscope images with rotational symmetry. *J. Mol. Biol.* **60**, 123–130.

Crowther, R. A., Padrón, R., and Craig, R. (1985) The arrangement of the heads of myosin in relaxed thick filaments from tarantula muscle. *J. Mol. Biol.* **184**, 429–439.

Guerrero, J. R., and Padrón, R. (1992) The substructure of the backbone of the thick filament from tarantula muscle. *Acta Microscopica* **1**, 63–83.

Guerrero, J. R., Granados, M., Alamo, L., Padrón, R., and Craig, R. (1992) Visualization of myosin helices in sections of rapidly frozen, relaxed tarantula muscle. *Biophys. J.* **61**, 301a.

Kensler, R. W., and Levine, R. J. C. (1982) An electron microscopic and optical diffraction analysis of the structure of *Limulus* telson muscle thick filaments. *J. Cell Biol.* **92**, 443–451.

Kensler, R. W., and Stewart, M. (1983) Frog skeletal muscle thick filaments are three-stranded. *J. Cell Biol.* **96**, 1797–1802.

Kensler, R. W., and Stewart, M. (1986) An ultrastructural study of cross-bridge arrangement in the frog thigh muscle thick filament. *Biophys. J.* **49**, 343–351.

Lehman, W., and Szent-Györgyi, A. G. (1975) Regulation of muscular contraction. Distribution of actin control and myosin control in the animal kingdom. *J. Gen. Physiol.* **66**, 1–30.

Lepault, J., Erk, I., Nicolas, G., and Ranck, J. L. (1991) Time-resolved cryo-electron microscopy of vitrified muscular components. *J. Microsc.* **161**, 47–57.

Padrón, R., and Craig, R. (1989) Disorder induced in non-overlap myosin cross-bridges by loss of adenosine triphosphate. *Biophys. J.* **56**, 927–933.

Padrón, R., Alamo, L., Caputo, C., and Craig, R. (1988) A method for quick-freezing live muscles at known instants during contraction with simultaneous recording of mechanical tension. *J. Microsc.* **151**, 81–102.

Padrón, R., Panté, N., Sosa, H., and Kendrick-Jones, J. (1991) X-ray diffraction study of the structural changes accompanying phosphorylation of tarantula muscle. *J. Musc. Res. Cell Motil.* **12**, 235–241.

Padrón, R., Granados, M., Alamo, L., Guerrero, J. R., and Craig, R. (1992) Visualization of myosin helices in sections of rapidly frozen relaxed tarantula muscle. *J. Struct. Biol.* **108**, 269–276.

Reynolds, E. S. (1963) The use of lead citrate at high pH as an electron-opaque stain in electron microscopy. *J. Cell Biol.* **17**, 208–213.

Stewart, M., and Kensler, R. W. (1986) Arrangement of myosin heads in relaxed thick filaments from frog skeletal muscle. *J. Mol. Biol.* **192**, 831–851.

Stewart, M., Kensler, R. W., and Levine, R. J. C. (1981) Structure of *Limulus* telson muscle thick filaments. *J. Mol. Biol.* **153**, 781–790.

Stewart, M., Kensler, R. W., and Levine, R. J. C. (1985) Three-dimensional reconstruction of the thick filaments from *Limulus* and scorpion muscle. *J. Cell Biol.* **101**, 402–411.

Vibert, P., and Craig, R. (1983) Electron microscopy and image analysis of myosin filaments from scallop striated muscle. *J. Mol. Biol.* **165**, 303–320.

Vibert, P. (1992) Helical reconstruction of frozen-hydrated scallop myosin filaments. *J. Mol. Biol.* **223**, 661–671.

Wray, J. S. (1982) Organization of myosin in invertebrate thick filaments. *In* Twarog, B. M., Levine, R. J. C., and Dewey, M. M. (Eds.), Basic Biology of Muscles: A Comparative Approach, pp. 29–36, Raven, New York.